UNIVERSITY OF LEEDS

This is a repository copy of *Climate and fragmentation affect forest structure at the southern border of Amazonia*.

White Rose Research Online URL for this paper:
http://eprints.whiterose.ac.uk/128852/

Version: Accepted Version

Article:

Reis, SM, Marimon, BS, Marimon Junior, BH et al. (9 more authors) (2018) Climate and fragmentation affect forest structure at the southern border of Amazonia. Plant Ecology and Diversity, 11 (1). pp. 13-25. ISSN 1755-0874

https://doi.org/10.1080/17550874.2018.1455230

© 2018 Botanical Society of Scotland and Taylor & Francis. This is an Accepted Manuscript of an article published by Taylor & Francis in Plant Ecology & Diversity on 25 Apr 2018, available online: http://www.tandfonline.com/10.1080/17550874.2018.1455230. Uploaded in accordance with the publisher's self-archiving policy.

Reuse
Items deposited in White Rose Research Online are protected by copyright, with all rights reserved unless indicated otherwise. They may be downloaded and/or printed for private study, or other acts as permitted by national copyright laws. The publisher or other rights holders may allow further reproduction and re-use of the full text version. This is indicated by the licence information on the White Rose Research Online record for the item.

Takedown
If you consider content in White Rose Research Online to be in breach of UK law, please notify us by emailing eprints@whiterose.ac.uk including the URL of the record and the reason for the withdrawal request.

White Rose
university consortium
Universities of Leeds, Sheffield & York

eprints@whiterose.ac.uk
https://eprints.whiterose.ac.uk/

Climate and fragmentation affect forest structure in the southern border of Amazonia

Simone Matias Reis[a,b], Beatriz Schwantes Marimon[b,c,*], Ben Hur Marimon Junior[b,c], Paulo S. Morandi[a,b], Edmar Almeida de Oliveira[b], Fernando Elias[c], Eder Carvalho das Neves[c], Bianca de Oliveira[c], Denis Silva Nogueira[c], Ricardo Keichi Umetsu[c], Ted R. Feldpausch[c,d] and Oliver L. Phillips[a]

[a]School of Geography, University of Leeds, Leeds, United Kingdom; [b]Programa de Pós-Graduação da Rede de Biodiversidade e Biotecnologia da Amazônia Legal (BIONORTE), Universidade do Estado de Mato Grosso–Universidade Federal do Amazonas, Nova Xavantina, Mato Grosso, Brazil; [c]Universidade do Estado de Mato Grosso, Programa de Pós-graduação em Ecologia e Conservação, Nova Xavantina, MT, Brazil; [d]University of Exeter, Geography, College of Life and Environmental Sciences, Exeter, United Kingdom

*Corresponding author. Email: biamarimon@unemat.br

Abstract

Background: The remaining forests in the extensive contact zone between southern Amazonia (seasonal rain forest) and the Cerrado (savanna) biomes are at risk due to intense land-use and climate change.

Aims: To explore the vulnerability of these transitional forests to changes in land use and climate, we evaluated the effects of fragmentation and climatic variables on forest structure.

Methods: We measured the diameter and height of 14,185 trees with diameter $\geq$ 10 cm at 24 forest plots distributed over an area of 25,000 km^2. For each plot, we obtained data on contemporary fragmentation and climatic variables.

Results: Forest structure variables (height, diameter, height:diameter allometry, biomass) varied significantly both within and among plots. The height, H:D and biomass of trees were positively correlated with annual precipitation and fragment area.

Conclusions: The association between forest structure and precipitation indicates that these forests plots are likely to be vulnerable to dry season intensification anticipated for the southern edge of the Amazon. Additionally, the reduction in the fragment area may contribute to reductions in forest biomass and tree height, and consequently ecosystem carbon stocks. Given the likely susceptibility of these forests, urgent conservation action is needed to prevent further habitat degradation.

Keywords: allometry; Amazon arc of deforestation; biomass; climate change; habitat fragmentation; precipitation; stem diameter; tree height; transition zone

Introduction

Across the Earth’s biomes, environmental conditions are expected to be more variable close to the edges than in the core area of each biome, posing potentially ecological and evolutionary challenges to biota towards their biogeographical edges (Safriel et al. 1994; Kark and van Rensburg 2006; Kark et al. 2008). This may be particularly the case in regions subject to rapid environmental change, of which perhaps the most extreme example are the forests of the southern edge of the Amazon rain forest biome, an area affected by high deforestation rates and subject to significant recent and forecast climate change. Thus, here the advance of the agricultural frontier has already resulted in converting most forest to pasture and cropland, increasingly fragmenting the landscape over the last few decades (Alencar et al. 2004, 2015; Nogueira et al. 2008). The remaining forests are subject to recent climate change, including lengthening of the dry season and increasing incidence of strong droughts (Marengo et al. 2011; Gloor et al. 2015; Feldpausch et al. 2016), trends which are expected to intensify further (e.g. Boisier et al. 2015). The land surface temperature has been rising steadily recently, especially in the south and east of the Amazon region (Jiménez-Muñoz et al. 2013), and the effects of these climatic changes may be exacerbated by changes in land use (Aragão 2012; Silvério et al. 2015). Finally, research elsewhere in Amazonia clearly has indicated that the structure of the tropical forest vegetation is affected by both climate change (e.g. Phillips et al. 2010; Feldpausch et al. 2016) and fragmentation of habitats (e.g. Laurance et al. 1997, 2000; Laurance 2004).

Yet few studies have evaluated structural variation among the forests in the southern border region of the Amazon forest biome and its covariation with climate and landscape factors. Exceptions include one analysis of the effects of the interaction between droughts and wildfires on tree mortality at one experimental site (Brando et al.

2014), and a landscape study which showed that habitat fragmentation, combined with droughts, increased the susceptibility of the forests to fire (Alencar et al. 2015). We are not aware of a single study that has evaluated the effects of habitat fragmentation and different climate variables across the region's forests using direct, on-the-ground measurement of vegetation structural variables such as tree diameter, height, and biomass.

Habitat fragmentation, by decreasing fragment size and increasing forest edges and numbers of fragments, may modify the forest structure in the remaining fragments (Fahring 2003; Haddad et al. 2015). For example, fragment edges are subject to a greater incidence of insolation and increased velocity of winds, resulting in higher temperatures and a drier microclimate than the forest interior (D'Angelo et al. 2004; Laurance 2004; Haddad et al. 2015), which increases tree mortality rates, principally for larger trees (Laurance et al. 2000; Laurance 2004). The death of bigger trees reduces total biomass, height, mean diameter and basal area, especially in the smaller fragments and the areas closest to the forest edge, although with some mortality effects also propagating a few hundred meters into the forest (Laurance 2004; Haddad et al. 2015; Rocha-Santos et al. 2016). Recently, it has even been suggested, based on interpretation of pantropical satellite imagery, that in tropical forests the negative effects on standing biomass and forest structure penetrate as much as 1.5 km into forests (Chaplin-Kramer et al. 2015).

In addition to landscape-scale factors, regional climate is related to variation in the forest structure (e.g. Banin et al. 2015). For example, where precipitation and temperature are higher, forests generally have taller trees that accumulate more biomass (Koch et al. 2004; Way and Oren 2010; Feldpausch et al. 2011; Pan et al. 2013; Chave et al. 2014). However, in the very warmest forests the forest structural responses are unclear. There is some evidence that here plants may photosynthesise less and expend more energy on respiration, so potentially accumulating less biomass (Lloyd and Farquhar 2008; Lewis et al. 2013). However, the temperature sensitivity of key respiration processes appears to decline in warmer environments (Atkin et al. 2015, Heskel et al. 2016), rather than increasing exponentially as simple Q_{10} formulations in earlier global vegetation models suggested (Cox et al. 2000), suggesting that the overall sensitivity of biomass stocks to high temperatures might be weaker than many models indicated.

Extreme drought events may alter the forest structure. Drought causes mortality, principally in the bigger trees, which are more susceptible to damage in their vascular system (Phillips et al. 2010; Rowland et al. 2015; Bennett et al. 2015; Feldpausch et al. 2016). During drought events, tropical trees may also grow less (e.g. Worbes 1999; Doughty et al. 2015), and if droughts are prolonged or repeated forests eventually accumulate less biomass (Feldpausch et al. 2016; Rowland et al. 2015).

In the context of regional land-use and climatic changes in southern Amazonia, and the projected high regional climate sensitivity to global warming (IPCC 2015), it is therefore extremely important to understand how the forest structure is affect by abiotic factors. It may for example help to improve the conservation measures to protect the remaining forest fragments. In this study, we evaluated whether, and to what extent, climatic factors and fragmentation determine variation in the forest structure of the southern Amazon border. We assembled data from permanent plots established across the region close to the natural border of Amazonia with the neighboring Cerrado (savanna) biome, to test hypotheses related to the variation in the forest structure and the factors that determine this variation. We addressed two questions. First, does habitat fragmentation affect the forest structure? We expected that forest cover loss and forest plots present in smaller fragments and/or nearer the edge would have trees with lower height and smaller diameter stems, or with smaller height:diameter (H:D) allometric relationships and reduced biomass, since work elsewhere has shown mortality rates are greater in smaller, more edge-affected fragments, especially for bigger trees (e.g. Laurance et al. 1997, 1998, 2000; Laurance 2004; Chaplin-Kramer et al. 2015). Second, how does the forest structure vary in relation to the climate? We expected that the height and the diameter of stems, the H:D ratio, and biomass were all greater in forest plots that have greater precipitation, and consequently less deficit water, since the greater water availability favours the height growth of the trees, accumulating more biomass (e.g. Feldpausch et al. 2011; Pan et al. 2013; Chave et al. 2014).

Materials and methods

Study area

We studied 24 forest plots distributed in the so-called ‘arc of deforestation’ (Nogueira et al. 2008) over an area of ca. 25,000 km^2 (Figure 1 and Table 1). The regional climate is of the Aw (tropical with dry winters) and Am (tropical monsoon) types in the Köppen classification system (Alvares et al. 2013), and originally supported evergreen or semi-evergreen forest vegetation in all cases. Mean annual precipitation and temperature range from 1511 to 2353 mm and from 24.1 to 27.3 °C, respectively (Table 1).

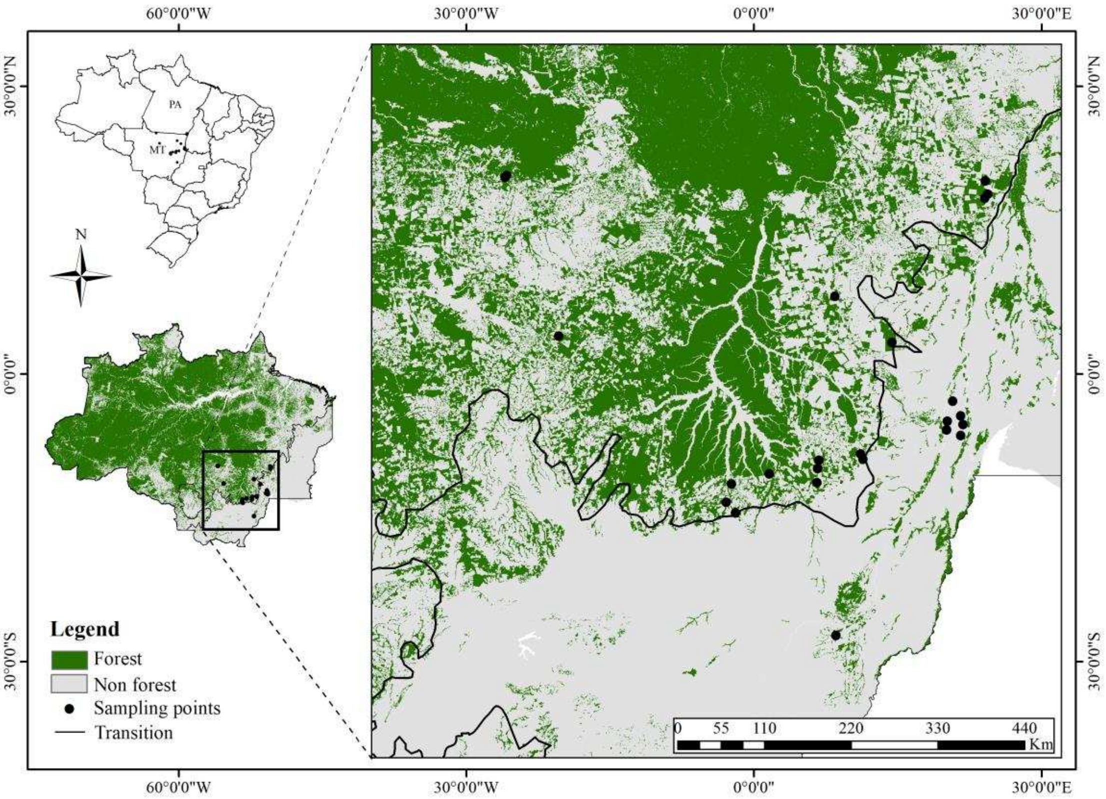

Figure 1. Location of the forests sampled in the southern Amazon border, between eastern and northern Mato Grosso and southern Pará, Brazil, showing the approximate biome boundaries based in IBGE (2004). The classification of forest and no forest was based on the PRODES (Amazon Deforestation Monitoring Project) (INPE 2017). All plots sampled lie within mature, evergreen or semi-evergreen forest fragments.

Table 1. Characteristics of plots sampled in different tropical forest ecosystems at the southern Amazon border. FA, fragment area; DE, distance to the forest edge; Prec, total mean annual precipitation; Temp, mean annual temperature; TB, total above-ground biomass per hectare; PP, private properties; and CU, conservation unit. In this study, we used codes (‘Plot code’) to represent the different types of vegetation: FEP, floresta estacional perenifólia (seasonal evergreen forest), FTP, floresta estacional perenifólia em terra preta de índio (seasonal evergreen forest on anthropogenic black earth); FES,

floresta estacional semidecidual (seasonal semi-deciduous forest); FOA, floresta ombrófila aberta (open rainforest); and FSI, floresta sazonalmente inundável (seasonally flooded forest). Equivalent forest plot codes are given to indicate equivalency to those codes used in the ForestPlots.net database (Lopez-Gonzalez et al. 2011) where the data have been deposited.

Plot Code	Forest plot code	Geographical coordinate	Local	AF (ha)	DE (m)	Prec (mm)	Temp (°C)	TB (Mg)
FEP-01	FLO-01	-12.8S and -51.9W	PP	870	1,030	1613	25.5	111.1
FEP-02	FLO-02	-12.8S and -51.9W	PP	2,035	1,000	1621	25.6	144.7
FEP-03	TAN-02	-13.1S and -52.4W	PP	8,432	990	1625	24.9	143.5
FEP-04	TAN-03	-12.8S and -52.3W	PP	16,901	520	1679	25.1	127.4
FEP-05	TAN-04	-12.9S and -52.4W	PP	16,901	329	1662	25	138.3
FEP-06	FRP-01	-11.5S and -51.5W	PP	45,459	3,600	1634	26.9	135.1
FEP-07	POA-01	-11.0S and -52.2W	PP	9,789	1,180	1772	26.1	140.1
FES-01	VCR-02	-14.8S and -52.2W	PP	4,968	1,350	1511	25.2	196.8
FES-02	GAU-02	-13.4S and -53.3W	PP	3,499	160	1701	24.1	91.7
FES-03	SAT-01	-9.8S and -50.5W	PP	17,624	90	1821	26.7	121.8
FES-04	SAA-01	-9.8S and -50.4W	PP	13,039	860	1815	26.8	187.7
FES-05	SAA-02	-9.6S and -50.4W	PP	15,680	2,980	1778	26.6	166.3
FOA-01	SIP-01	-11.4S and -55.3W	PP	12,066	900	1848	25.1	79.2
FOA-02	ALF-01	-9.6S and -55.9W	CU	17,628	5,440	2350	25.5	98.8
FOA-03	ALF-02	-9.6S and -55.9W	CU	17,628	5,410	2353	25.6	160.5
FSI-01	PEA-01	-12.1S and -50.8W	CU	21	1	1631	27.3	133.7
FSI-02	PEA-02	-12.3S and -50.7W	CU	378	1	1637	27.2	154.7
FSI-03	PEA-03	-12.4S and -50.9W	CU	164	1	1621	27.1	131.4
FSI-04	PEA-04	-12.4S and -50.7W	CU	605	1	1637	27.1	210.4
FSI-05	PEA-07	-12.5S and -50.9W	CU	5	1	1621	27.1	226.8
FSI-06	PEA-08	-12.5S and -50.7W	CU	8	1	1632	27	222.5
FTP-01	GAU-04	-13.1S and -53.3W	PP	234	150	1795	24.7	145.8
FTP-02	GAU-05	-13.0S and -52.9W	PP	29,560	2,720	1757	24.9	250.2
FTP-03	GAU-06	-13.3S and -53.4W	PP	85	80	1729	24.7	176.9

Forest fragments

The largest and best preserved regional fragments of mature forests were selected for the study, using Google Earth imagery in order to capture regional variation in floristics and physiognomy, and with at least three plots for each forest type. All forest fragments are surrounded by extensive cattle-ranching or soybean fields. The fragments surveyed varied in size from 5 to 45,459 ha (Table 1).

Forest structure

In each fragment we established an inventory plot of 1 ha, which was subdivided into 25 contiguous subplots of 20 m x 20 m. The forest plots were established between 2008 and 2016 within the private properties and in conservation units; locations varied between 1 and 5440 m from the nearest edge of the fragment. Six plots were seasonally flooded (Table 1) and occasionally affected by fire; the others have no recent record of fire and were either on anthropogenic black earth (terra preta de índio), open rain forests, seasonal evergreen forests, or seasonal semi-deciduous forests (Table 1). For this study, we used the latest available censuses between 2013 and 2016.

We identified and tagged all the woody individuals with a diameter at breast height (1.3 m) of ≥ 10 cm, for a total of 14,185 (range = 338-1599; standard deviation = 31) trees and at least 410 (range = 9-135; standard deviation = 256) taxa identified to species level. We identified species in the field or by comparison of collections with herbarium (NX, UFMT, UB and IAN) material of known identity, and with the help of specialists. After identification, the material was incorporated into Herbarium NX, Nova Xavantina, Mato Grosso (Coleção Zoobotânica James Alexander Ratter). We determined the classification of families based on APG III (Angiosperm Phylogeny Group 2009) and reviewed and updated the nomenclature of the taxa using the Lista de Espécies da Flora do Brasil (http://floradobrasil.jbrj.gov.br/2015).

We measured the diameter of each tree following standard protocols of the RAINFOR network (http://www.rainfor.org/). We measured the total height using a

Leica DISTO laser measurement device. Data were deposited in the ForestPlots.net forest monitoring database (Lopez-Gonzalez et al. 2011).

Habitat fragmentation

To evaluate the effect of habitat fragmentation on forest structure, we measured distance from each plot to the forest edge, the size of each fragment and the forest cover in surrounding landscapes. Whenever possible we measured the distance to the nearest edge in the field. When this was not possible, we estimated this value using Google Earth, which provided a spatial resolution of approximately 20 to 30 m depending on available imagery, and based on our own detailed knowledge, having explored the local context of each plot on foot. In our definition of forest habitat edge, we included all other vegetation and land-use such as plantations, pastures, and roads at least 25 m wide, as well as natural grasslands in the six floodplain forests.

We calculated the area of the fragment where each plot was located using Google Earth and ZONUM software (http://zonums.com/online/kmlArea/). These edge and fragment data were collected at the closest possible date to the field sampling and in no case were they collected more than 2 years after the last forest census.

We calculated the percentage of forest cover surrounding each plot using buffers of radius size of 1000 m (314 ha), following recommendations of Rocha-Santos et al. (2016). For this we used the land-based metrics in the Fragstats software, that computes descriptors of forest patch and landscape attributes (McGarigal and Cushman 2002).

Climate variables

To evaluate the climate effect on the forest structure, we obtained data on 19 bioclimatic variables (Table S1) from the WorldClim 1.4 database, with a horizontal resolution of ca. 1 km (Hijmans et al. 2005). We also used data from the Tropical Rainfall Monitoring Mission (TRMM) (NASA 2012) to derive the mean of the annual maximum climatological water deficit (MCWD) (Aragão et al. 2007) between January 1999 and December 2011, including the droughts of 2005, 2007 and 2010 (Figure S2). To estimate this, we first calculated MCWD for each year, and then took the mean of all years. MCWD was defined as the most negative value of climatological water deficit (precipitation lower than evapotranspiration) among all the months in each year.

Data analysis

In each plot, we calculated the minimum, maximum, median, and 95 percentile of tree diameter (D), height (H) and their allometric (H:D) relationship. We also calculated the weighted Lorey's height values, based on basal area per subplot, using the equation

$$\sum AB_i * H_i / \sum AB_i,$$

where AB_i is the basal area of an individual and H_i is its height (e.g. Saatchi et al. 2011). To evaluate the H:D relationship, independently of disturbance, such as the damage caused by recently-opened clearings, we excluded from the analyses all trees with broken stems or those with more than 50% of the crown broken off.

We also calculated the mean, median, and total biomass of trees per plot. We estimated the biomass (B) based on the Pantropical model revised by Chave et al. (2014), which is derived from the equation in Chave et al. (2005), that is,

$$B = 0.0673 \text{ x } (\rho D^2 H)^{0.976},$$

where D is the diameter in cm, H is the total height of the tree in m, and ρ is the density of the wood. We obtained wood density values from the ForestPlots database (https://www.ForestPlots.net/). We chose this equation to calculate the biomass because it is the most robust approach, given that it takes into consideration the diameter and height of each tree.

We developed a correlation matrix of the Kendall's tau values of the environmental and forest structure variables mentioned above (Table S3). Multiple variables share similar source data, leading to high correlation amongst them, so we excluded those with greatest correlations ($r > 0.7$) to avoid repetition of largely redundant forest structure and climate variables (Tables S3 and S4). For all variables, the maximum values and the 95 percentiles were highly correlated; we included only the 95 percentile in order to avoid the influence of outliers. Finally, we excluded predictor variables that correlated poorly ($r < 0.1$) with the vegetation descriptors (Tables S3 and S4).

To verify possible differences among all forest plots in the structural variables (95 percentiles of the D, H and H:D, and mean B), we applied the Kruskal-Wallis analysis of variance with the Dunnett post hoc test and a Bonferroni correction (Zar 2010).

We evaluated the influence of habitat fragmentation and climatic variables on forest structure using simple correlation and Generalised Linear Models (GLM). We also included in the models the forest type for each forest plot. Simple correlation showed that, six seasonally flooded plots and two plots on anthropogenic black earth were unduly influential, with extreme structure and covarying extreme climatic and fragmentation conditions. To avoid these outliers driving the regional results we excluded them from the GLM and correlation analyses described above.

To build the GLM, we first standardised the data and removed the collinearities on the basis of Variance Inflation Factors (VIFs) of less than 10 (Quinn and Keough 2002). We conducted model selection using the Akaike's Information Criterion (AIC), with a model considered to be the best if it had the lowest AIC value (Barton 2016). To access the spatial autocorrelation in the residuals for each model we used Moran's I. Here, no spatial dependence was detected among plots, indicating that the data were not spatially structured (Figure S5). Thus, we considered the plots as independent samples in our subsequent analyses.

We conducted the analyses using SAM 4.0 program (Rangel et al. 2010) and R 2.15.1 (R Core Team 2012). The applied R packages were vegan (Oksanen et al. 2016), spdep (Bivand et al. 2013), spacemakeR (Dray 2013), MuMIn (Barton 2016) and packfor (Dray et al. 2016). We adopted a 5% significance level for all analyses and used 999 randomisations for the permutation methods.

Results

Forest structure

In general, the three open rainforest plots (FOA-01-03), a forest plot on anthropogenic black earth (FTP-01), were significantly taller than the six seasonally flooded forest plots (FSI-01-06), three seasonal semi-deciduous forest (FES-01-02-05) (Figure 2 and Table S6) and like the other 11 forest plots (FEP-01-07; FES-03-04 and FTP-02-03). The H:D ratio varied in a similar fashion to tree height, with the lowest ratios (i.e., the lowest heights for a given diameter) being recorded in two of the seasonally flooded forest plots (FSI-05 and FSI-06). Tree diameter and biomass did not vary systematically among the plots, except for FSI-03, which had lower diameter and biomass than the most of others plots (Figure 2).

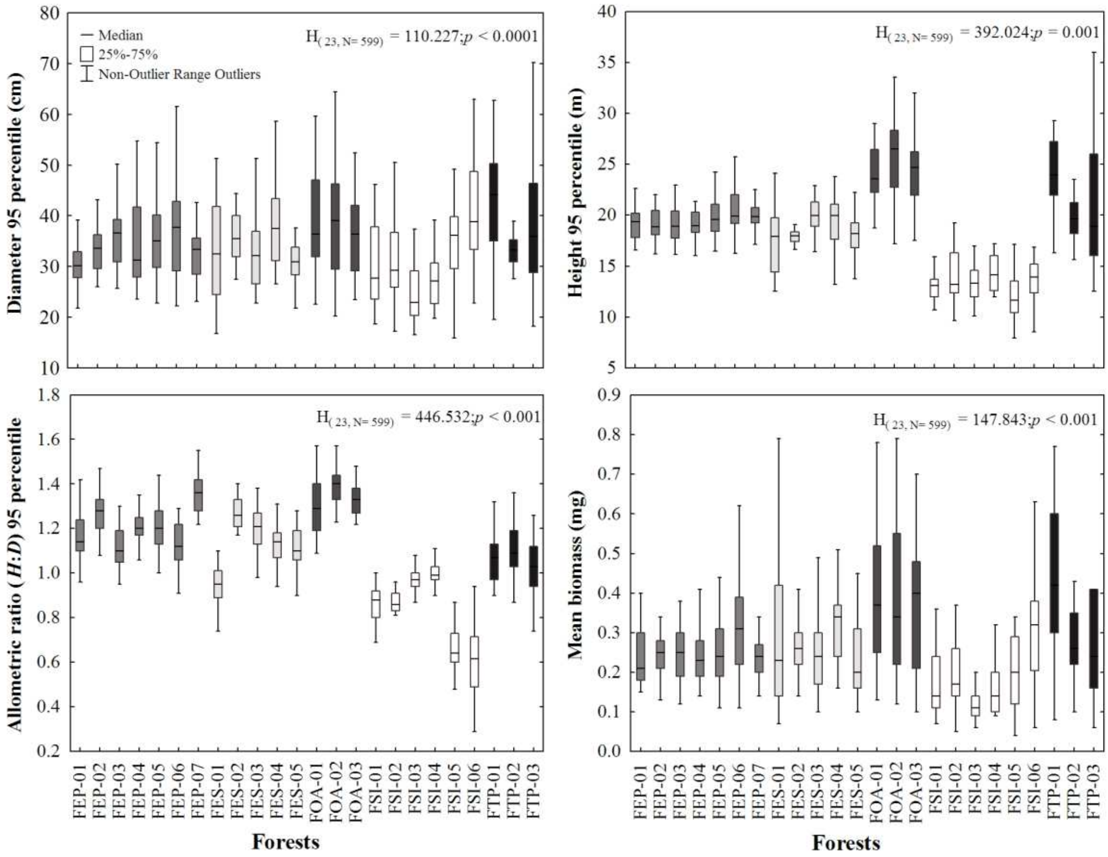

Figure 2. Variation in the vertical structure of forests at the southern Amazon border. Box-plots show subplot-level values in each location, statistical comparisons are made for among-forest analyses based on the non-parametric Kruskal-Wallis test (H). The complementary pair-wise analysis of forest structure is provided in Table S7. ■ = FTP (seasonal evergreen forest on anthropogenic black earth), ▩ = FOA (open rainforest), ▨ = FEP (seasonal evergreen forest), ░ = FES (seasonal semi-deciduous forest), □ = FSI (seasonally flooded forest).

Relationship between forest structure, fragmentation and climate variables

The structural variables were associated with the precipitation and with fragment area and distance from the edge (Figure 3 and Table 2). Tree height, allometry (H:D) and biomass all correlated positively with precipitation and fragment area (Figure 3). Tree height also correlated with the MCWD (Figure 3). Tree diameter did not correlate with any of the variables. Additionally, the precipitation and MCWD correlated positively with the fragment area ($P < 0.05$; Kendal's $\tau = 0.44$ and 0.60, respectively).

Table 2. The relationship between environmental variables and forest structure, using generalised linear models, of the southern Amazonia forests, Brazil. DE, distance to the edge; PrecWM, precipitation of wettest month; H:D, allometric H:D ratio; FES, seasonal semi-deciduous forest-plots; FOA, open rainforest-plots. Significant effects ($P \leq 0.05$) are shown in bold type.

	Factors	Estimate	Standard	t	P
Height 95 percentile					
	Intercept	-0.276	0.109	-2.531	**0.003**
	FES	-0.008	0.161	-0.050	0.961
	FOA	1.392	0.328	4.249	**0.001**
	PrecWM	0.431	0.140	3.082	**0.010**
Diameter 95 percentile					
	Intercept	-0.356	0.290	-1.228	0.243
	FES	0.039	0.445	0.089	0.931
	FOA	1.715	0.530	3.237	**0.007**
H:D 95 percentile					
	Intercept	<0.001	0.174	<0.001	1.000
	DE	-0.785	0.302	-2.597	**0.023**
	PrecWM	1.260	0.302	4.167	**0.001**
Mean biomass					
	Intercept	-0.540	0.166	-3.249	**0.007**
	FES	0.244	0.257	0.949	0.361
	FOA	2.291	0.303	7.555	**<0.001**

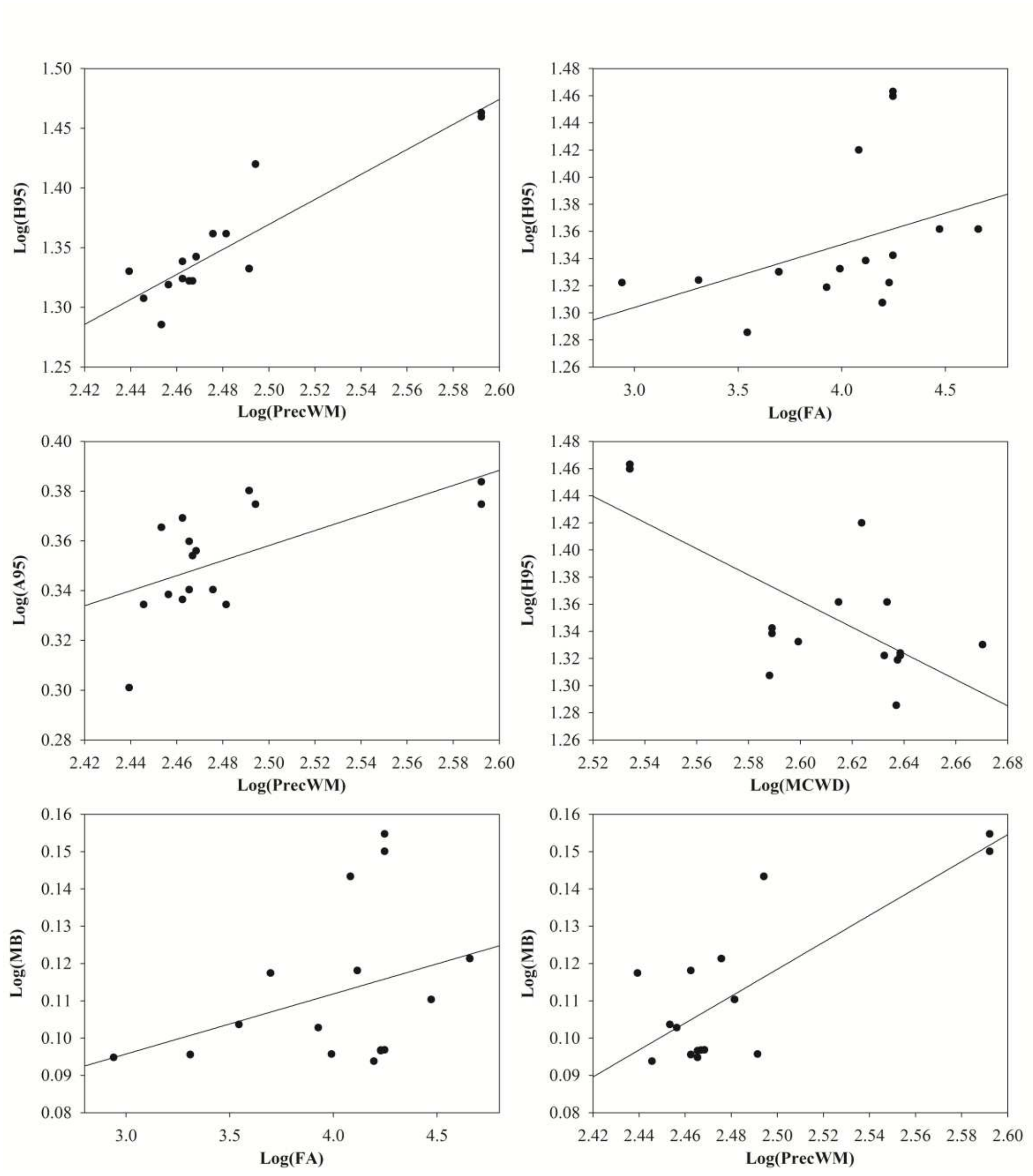

Figure 3. Significant ($P \leq 0.05$) relationships between forest structure and climatic and fragmentation variables of the southern Amazon border forest plots. H95 = height 95 percentile, A95 = allometric ratio (H:D) 95 percentile, MB = mean biomass (Mg), FA = fragment area (ha), PrecWM = precipitation of wettest month (mm), MCWD = maximum climatological water deficit (mm).

Based on the best GLM models for each forest structure variable, forest type and precipitation were most related to tree height (Table 2). Forest type was also a strongly related to tree diameter and biomass. Annual mean precipitation and distance from the edge were important factors for mean plot H:D (Table 2). The percentage of forest cover around each plot was not selected in the best models and was not correlated with any forest structure variables. All plots presented more than 50% forest cover in surrounding landscapes.

Precipitation and MCWD were not selected in the same model, indicating that each had similar (but inverse) effects on forest structure. Thus, all structural parameters affected positively by precipitation (Table 2) are affected negatively by moisture stress (MCWD) (Table S7).

Discussion

Our results show that the forests of the southern border zone of Amazonia vary remarkably in their structure, principally in terms of their tree height and tree height:diameter ratio. Most of the structural variation in these forests was statistically related to fragment area and precipitation, supporting our overall expectations and largely consistent with our hypotheses. Here we briefly first discuss this overall variability and its potential ultimate drivers, before proceeding to discuss the results in more detail.

Structural variability of the forests of the southern Amazon border zone

Our general expectation was that climatic variation in the region would be a fundamental determinant of the variability in forest structure here, principally because drought events and seasonality may be more intense at the southern border in relation to the core area of the Amazonas basin with evergreen non-seasonal rain forests (Lewis et al. 2011). In particular, water deficit may kill large trees (McIntyre et al. 2015), taller trees tend to be most affected by these conditions (Rowland et al. 2015). As these trees die and break-up or fall, large clearings are opened, favouring the establishment of species of different ecological groups (Lawton and Putz 1988). The frequent formation of clearings in these hyperdynamic transitional forests, as documented by Marimon et al. (2014), may thus also contribute to the structural variability found here. Finally, the forests of the southern border of the Amazon are located within a mosaic of vegetation types with many species typical of the adjacent biomes (Ratter et al. 1973), which may have a direct influence on the structural diversity of these forests.

Seasonally flooded forest plots

The lowest height and H:D allometric ratio in the seasonally flooded forest plots may be explained by their smaller fragment size and proximity to edges. These factors as well as higher temperatures and lower precipitation (Table 1) may intensify the fire effects. Fires in the wider grassland matrix can penetrate into forest fragments and increase tree mortality, as observed in a recent study in these forest plots (Maracahipes et al. 2014). It therefore appears likely that the combined effects of reduced fragment area and precipitation and higher temperatures, together with fire and its potential interactions with droughts (Brando et al. 2014), contribute to forest structure here.

Response of the forest structure to the fragmentation and climate variables

Temperature appears to be an important factor determining the height of the trees worldwide, including potentially in tropical forests (Koch et al. 2004; Way and Oren 2010; Feldpausch et al. 2011; Lines et al. 2012; Pan et al. 2013), but here the absence of a clear statistical relationship between structure and temperature ($P > 0.05$, Kendal's $\tau = 0.31$) suggests it is not critical at the southern Amazon transition zone. Rather, in our study the greater forest heights, H:D ratio and biomass that were observed with increasing precipitation suggest water supply is the dominant climate control on forest structure, and is consistent with some work elsewhere in the tropics (e.g. Alvarez et al. 2017), given especially that tropical plants tend to grow faster and taller as water is more available (Vlam et al. 2014; Givnish et al. 2014). In addition to apparent effects of annual rainfall, we also found that climatological water deficit was associated with reduced investment by the trees in height growth, consistent with the hypothesis that tree height is constrained by the availability of water (Ryan et al. 2004; Givnish et al. 2014). A significant positive correlation was also found between precipitation and tree height along a precipitation gradient in Australia, which Givnish et al. (2014) related to the increase in leaf area and rates of photosynthesis with increasing precipitation.

The negative correlation between the cumulative water deficit and tree height may be related to the mortality of the largest individuals during extreme drought events (Phillips et al. 2010). Such droughts have been directly observed in the study region in 2005, 2007, and 2010 (e.g. Brando et al. 2014), and these have indeed tended to kill larger trees (Phillips et al. 2010; Feldpausch et al. 2016), as is often the case with droughts in other tropical forests (Bennett et al. 2015). In Amazonia, recent strong droughts appear also to be a major cause of the recent basin-wide increase in tree mortality rates (Phillips et al. 2009; Brienen et al. 2015). In the near future, more frequent extreme droughts, especially if combined with warming of the Amazon region and thermal peaks in El Niño events such as in 2015-16 (Jiménez-Muñoz et al. 2016), may therefore have profound implications for the forest structure of the southern Amazon border, located as they are in a region that is already naturally close to their distributional and hydraulic limits. In this scenario, large trees are more susceptible to damage to the xylem, which can ultimately result in the death of the plant (e.g. McIntyre et al. 2015) and eventually lead to forests of lower stature (McDowell et al. 2008; Rowland et al. 2015). Trees being smaller in drier areas with greater water deficiency is directly be related to conservative modifications in the hydraulic structure of the plants under hydrological stress to avoid embolism (e.g. Lines et al. 2012, Claeys and Inzé 2013). Thus, as have recently argued in both tropical and temperate zone contexts (e.g. Stegen et al. 2011; Banin et al. 2012; McIntyre et al. 2015) it is likely that trees in forests subject either to more extreme climatic events, or to more disturbance (including seasonally flooded habitats), or both, will in general tend to be shorter at a given diameter in order to avoid risks of hydraulic and/or mechanical failure, whereas trees in forests with high rainfall, such as our FOA-01 and FOA-02, will have greater heights and hence greater biomass.

Besides the correlation with the climatic variables, both height and the biomass of trees were positively correlated with fragment area. This result may be related to the incidence of wind in smaller fragments which have a higher proportion of forest edge (D'Angelo et al. 2004; Laurance 2004; Haddad et al. 2015). These disturbances are known to be able to generate high mortality, especially of the tallest trees (Laurance et al. 2000; Laurance 2004), and consequently in our dataset such edgegenerated disturbances may have affected the height and biomass of trees. Elsewhere, local climatic changes as a result of fragmentation can reduce the density and diversity of species (Mantyka-Pringle et al. 2012). Such effects can also increase the susceptibility of fragmented forest structure and their biota to fire (Laurance and Williamson 2001; Laurance 2004). In the southern Amazon region, these different effects are all likely to be relevant, but clearly further analysis is needed, including long-term monitoring evaluation of the climatic and dynamic processes in these forests.

Conclusions

Our analysis across different locations, spanning a large part of the southern Amazon zone, suggests climate sensitivity in forest structure here. Climate change, and especially any reduction in annual or seasonal precipitation, is thus likely to have a significant effect on the forest structure in the southern border of the Amazon. Secondly, our results also suggest that the effects of reduction in the annual precipitation may be further exacerbated in smaller fragments. This suggests that habitat fragmentation may intensify the negative effects of climate change and burning in forests in the southern Amazon border, resulting in a substantial risk of increases in tree mortality. Given the likely susceptibility of the remaining southern Amazon border forests to environmental change, strong conservation strategies are urgently needed to guarantee the persistence of these habitats, especially for the smaller fragments and those close to agricultural frontiers.

Acknowledgements

We are grateful to the team of the Laboratório de Ecologia Vegetal - Plant Ecology Laboratory at the UNEMAT campus in Nova Xavantina, especially to Henrique Augusto Mews, Nayane Cristina Prestes, Ana Paula Gomes da Silva, Laís Fernandes de Souza Neves, Mônica Forsthofer and Leonardo Maracahipes, for help in collecting field data. We also thank the National Council for Scientific and Technological Development (CNPq) for financial support of the projects PELD "Cerrado-Amazon Forest Transition: ecological and socio-environmental bases for Conservation" (stage II) - process nr. 403725/2012-7), PVE "special visiting researcher" (401279/2014-6), PPBIO "Phytogeography of the Amazon-Cerrado Transition Zone" (457602/2012-0) and FAPEMAT – Fundação de Amparo à Pesquisa do Estado de Mato Grosso (164131/2013). We also thank CNPq for research productivity grants to B.S. Marimon and B.H. Marimon Junior, a post-doctoral scholarship to D. Nogueira, and international doctoral grants to S.M.A. Reis and P.S. Morandi. We are also grateful to CAPES and FAPEMAT for scholarships to S.M.A. Reis, P.S. Morandi, F. Elias, E.A. Oliveira and E.C. Neves.

Notes on contributors

Simone Matias Reis is a Ph.D. student focussing on the effects of biotic and abiotic factors on forest structure in the southern border of Amazonia.

Beatriz Schwantes Marimon is professor and an ecologist with experience in working with structure and dynamics of different vegetation types of the southern Amazon boundaries in Central Brazil. Her current work focuses on ecology and management of forests in the transition zone between Cerrado and Amazon forest biomes, and currently has great interest in understanding changes in tropical plants communities as a result of climate change.

Ben Hur Marimon-Junior is professor. He has experience in forest ecology, studying biogeochemical cycles, carbon stocks, pyrogenic carbon in mineral nutrition of plants, biodiversity and ecosystem functions. His current work focuses on understanding changes in tropical plants communities as a result of climate change.

Paulo S. Morandi is a Ph.D. student focussing on structural patterns, diversity and distribution of species under the effect of environmental variables and vegetation succession in the Amazon-Cerrado transition.

Edmar Almeida de Oliveira is a Ph.D. student focussing on historical effect of soil disturbance and pyrogenic carbon on the composition and structure of forests in southern Amazonia.

Fernando Elias is a Ph.D. student focussing on the role of climate, land management and landscape on the resilience of secondary forests in the Amazon.

Eder Carvalho das Neves is M.Sc. student focussing on the physiology of forests in the Amazon-Cerrado transition.

Bianca de Oliveira is a biologist and conducted her master’s research on nutrient cycling in the Amazonia-Cerrado transition.

Denis Nogueira is a post-doctoral researcher focusing on forest dynamics of the Amazon-Cerrado transition in Mato Grosso.

Ricardo Keichi Umetsu is a lecturer. He has experience in environmental planning with emphasis on water resources, hydrographic basins, hydrogeochemistry of streams, plant ecology and landscape.

Ted R. Feldpausch is a lecturer in tropical ecology. His research focuses on the ecology and effects of global change on tropical forests.

Oliver L. Phillips is professor of tropical ecology. He leads the RAINFOR network of scientists in Amazonian forests.

References

Alencar A, Nepstad DC, McGrath D, Moutinho P, Pacheco P, Diaz MDCV, Soares Filho B. 2004. Desmatamento na Amazônia: indo além da "emergência crônica". Intituto de Pesquisa Ambiental da Amazônia, Belém.

Alencar AA, Brando PM, Asner GP, Putz FE. 2015. Landscape fragmentation, severe drought, and the new Amazon forest fire regime. Ecological Applications 25: 1493–1505.

Alvares CA, Stape JL, Sentelhas PC, de Moraes G, Leonardo J, Sparovek G. 2013. Köppen's climate classification map for Brazil. Meteorologische Zeitschrift 22: 711–728.

Álvarez-Dávila E, Cayuela L, González-Caro S, Aldana AM, Stevenson PR, Phillips O, Cogollo A, Peñuela MC, von Hildebrand P, Jiménez E, et al. 2017. Forest biomass density across large climate gradients in northern South America is related to water availability but not with temperature. PLOS ONE 12:e0171072.

Angiosperm Phylogeny Group. 2009. An update of the angiosperm Phylogeny group classification for the orders and families of flowering plants: APG III. Bot J Linn Soc 161: 105–121.

Aragao LEO, Malhi Y, Roman-Cuesta RM, Saatchi S, Anderson LO, Shimabukuro YE. 2007. Spatial patterns and fire response of recent Amazonian droughts. Geophysical Research Letters 34.

Aragão LE. 2012. Environmental science: The rainforest's water pump. Nature 489: 217–218.

Atkin OK, Bloomfield KJ, Reich PB, Tjoelker MG, Asner GP, Bonal D, Bönisch G, Bradford MG, Cernusak LA, Cosio EG, et al. 2015. Global variability in leaf respiration in relation to climate, plant functional types and leaf traits. New Phytologist 206:614-636.

Banin L, Feldpausch TR, Phillips OL, Baker TR, Lloyd J, Affum-Baffoe K, Arets EJMM, Berry NJ, Bradford M, Brienen RJW, et al. 2012. What controls tropical forest architecture? Testing environmental, structural and floristic drivers. Global Ecology and Biogeography 21: 1179–1190.

Banin LF, Phillips OL, Lewis SL. 2015. Tropical Forests. Routledge Handbook of Forest Ecology 5: 56–75.

Barton K. 2016. MuMIn: Multi-model inference. R package; [cited 2017 Fev 20]. Available from: https://cran.r-project.org/web/packages/MuMIn/MuMIn.pdf.

Bennett AC, McDowell NG, Allen CD, Anderson-Teixeira KJ. 2015. Larger trees suffer most during drought in forests worldwide. Nature plants 1: 15139.

Bivand RS, Hauke J, Kossowski T. 2013. Computing the Jacobian in Gaussian spatial autoregressive models: An illustrated comparison of available methods. Geographical Analysis 45: 150–179.

Boisier JP, Ciais P, Ducharne A, Guimberteau M. 2015. Projected strengthening of Amazonian dry season by constrained climate model simulations. Nature Climate Change 5: 656–660.

Brando PM, Balch JK, Nepstad DC, Morton DC, Putz FE, Coe MT, Silvério D, Macedo MN, Davidson EA, Nóbrega CC, et al. 2014. Abrupt increases in Amazonian tree mortality due to drought-fire interactions. Proceedings of the National Academy of Sciences 111: 6347–6352.

Brienen RJW, Phillips OL, Feldpausch TR, Gloor E, Baker TR, Lloyd J, Lopez-Gonzalez G, Monteagudo-Mendoza A, Malhi Y, Lewis SL, et al. 2015. Long-term decline of the Amazon carbon sink. Nature 519: 344–348.

Chaplin-Kramer R, Ramler I, Sharp R, Haddad NM, Gerber JS, West PC, Mandle L, Engstrom P, Baccini A, Sim S, et al. 2015. Degradation in carbon stocks near tropical forest edges. Nature communications 6.

Chave J, Andalo C, Brown S, Cairns MA, Chambers JQ, Eamus D, Folster H, Fromard F, Higuchi N, Kira T, et al. 2005. Tree allometry and improved estimation of carbon stocks and balance in tropical forests. Oecologia 145: 87–99.

Chave J, Réjou-Méchain M, Búrquez A, Chidumayo E, Colgan MS, Delitti WB, Duque A, Eid T, Fearnside PM, Goodman RC, et al. 2014. Improved allometric models to estimate the aboveground biomass of tropical trees. Global change biology 20: 3177–3190.

Claeys H, Inzé D. 2013. The agony of choice: how plants balance growth and survival under water-limiting conditions. Plant Physiology 162: 1768-1779.

Cox PM, Betts RA, Jones CD, Spall SA, Totterdell IJ. 2000. Acceleration of global warming due to carbon-cycle feedbacks in a coupled climate model. Nature 408: 184-187.

D'Angelo SA, Andrade ACS, Laurance SG, Laurance WF, Mesquita RCG. 2004. Inferred causes of tree mortality in fragmented and intact Amazonian forests. Journal of Tropical Ecology 20: 243–246.

Doughty CE, Metcalfe DB, Girardin CAJ, Amézquita FF, Cabrera DG, Huasco WH, Silva-Espejo JE, Araujo-Murakami A, da Costa MC, Rocha W, et al. 2015. Drought impact on forest carbon dynamics and fluxes in Amazonia. Nature 519: 78–82.

Dray S. 2013. spacemakeR: Spatial modelling. R package version 0.0-5/r113. https://R-Forge.R-project.org/projects/sedar/

Dray S, Legendre P, Blanchet G. 2016. packfor: Forward Selection with permutation (Canoco p. 46). R package version 0.0-8/r136. https://R-Forge.R-project.org/projects/sedar/

Feldpausch TR, Banin L, Phillips OL, Baker TR, Lewis SL, Quesada CA, Affum-Baffoe K, Arets EJMM, Berry NJ, Bird M, et al. 2011. Height-diameter allometry of tropical forest trees. Biogeosciences 8: 1081–1106.

Fahrig L. 2003. Effects of habitat fragmentation on biodiversity. Annual Review of Ecology, Evolution, and Systematics 34: 487–515.

Feldpausch TR, Phillips OL, Brienen RJW, Gloor E, Lloyd J, Lopez-Gonzalez G, Monteagudo-Mendoza A, Malhi Y, Alarcón A, Álvarez Dávila E, et al. 2016. Amazon forest response to repeated droughts. Global Biogeochemical Cycles 30: 1–19.

Givnish TJ, Wong SC, Stuart-Williams H, Holloway-Phillips M, Farquhar GD. 2014. Determinants of maximum tree height in Eucalyptus species along a rainfall gradient in Victoria, Australia. Ecology 95: 2991–3007.

Gloor M, Barichivich J, Ziv G, Brienen R, Schöngart J, Peylin P, Cintra BBL, Feldpausch T, Phillips O, Baker J. 2015. Recent Amazon climate as background for possible ongoing and future changes of Amazon humid forests. Global Biogeochemical Cycles 29: 1384–1399.

Haddad NM, Brudvig LA, Clobert J, Davies KF, Gonzalez A, Holt RD, Lovejoy TE, Sexton JO, Austin MP, Collins CD, et al. 2015. Habitat fragmentation and its lasting impact on Earth’s ecosystems. Science Advances 1: e1500052.

Heskel MA, O’Sullivan OS, Reich PB, Tjoelker MG, Weerasinghe LK, Penillard A, Egerton JJ, Creek D, Bloomfield KJ, Xiang J, et al. 2016. Convergence in the temperature response of leaf respiration across biomes and plant functional types. Proceedings of the National Academy of Sciences 113: 3832–3837.

Hijmans RJ, Cameron SE, Parra JL, Jones PG, Jarvis A. 2005. Very high resolution interpolated climate surfaces for global land areas. International journal of climatology 25: 1965–1978.

IBGE - Instituto Brasileiro de Geografia e Estatística. 2004. Área territorial brasileira; [cited 2017 Jun 25]. Available from: http://www.ibge.gov.br/

INPE – Instituto Nacional de Pesquisas Espaciais. 2017. Coordenação geral de observação da terra. Projeto PRODES: monitoramento da Floresta Amazônica Brasileira por Satélite; [cited 2017 Jun 29]. Available from: http://www.obt.inpe.br/prodes/index.php

IPCC - Intergovernmental Panel on Climate Change. 2015. Climate change 2014: mitigation of climate change. Cambridge: Cambridge University Press.

Jiménez-Muñoz JC, Mattar C, Barichivich J, Santamaría-Artigas A, Takahashi K, Malhi Y, Sobrino JA, van der Schrier G. 2016. Record-breaking warming and extreme drought in the Amazon rainforest during the course of El Niño 2015-2016. Scientific Reports 6: 33130.

Jiménez-Muñoz JC, Sobrino JA, Mattar C, Malhi Y. 2013. Spatial and temporal patterns of the recent warming of the Amazon forest. Journal of Geophysical Research: Atmospheres 118: 5204–5215.

Kark S, van Rensburg BJ. 2006. Ecotones: marginal or central areas of transition? Israel Journal of Ecology & Evolution 52: 29–53.

Kark S, Hadany L, Safriel UN, Noy-Meir I, Eldredge N, Tabarroni C, Randi E. 2008. How does genetic diversity change towards the range periphery? Evolutionary Ecology Research 10: 391–414.

Koch GW, Sillett SC, Jennings GM, Davis SD. 2004. The limits to tree height. Nature 428: 851–854.

Laurance WF, Ferreira LV, Rankin-de Merona JM, Laurance SG. 1998. Rain forest fragmentation and the dynamics of Amazonian tree communities. Ecology 79: 2032–2040.

Laurance WF, Laurance SG, Ferreira LV, Merona JMR, Gascon C. 1997. Biomass Collapse in Amazonian Forest Fragments. Science 278: 1117–1118.

Laurance WF, Delamônica P, Laurance SG, Vasconcelos HL, Lovejoy TE. 2000. Conservation: rainforest fragmentation kills big trees. Nature 404: 836–836.

Laurance WF, Williamson GB. 2001. Positive feedbacks among forest fragmentation, drought, and climate change in the Amazon. Conservation Biology 15: 1529–1535.

Laurance WF. 2004. Forest-climate interactions in fragmented tropical landscapes. Philosophical Transactions of the Royal Society of London B: Biological Sciences 359: 345–352.

Lawton RO, Putz FE. 1988. Natural disturbance and gap-phase regeneration in a wind-exposed tropical cloud forest. Ecology 69: 764–777.

Lewis SL, Brando PM, Phillips OL, van der Heijden GM, Nepstad D. 2011. The 2010 amazon drought. Science 331: 554-554

Lewis SL, Sonké B, Sunderland T, Begne SK, Lopez-Gonzalez G, van der Heijden, GM, Phillips OL, Affum-Baffoe K, Baker TR, Banin L, et al. 2013. Above-ground biomass and structure of 260 African tropical forests. Philosophical Transactions of the Royal Society B 368: 20120295.

Lines ER, Zavala MA, Purves DW, Coomes DA. 2012. Predictable changes in aboveground allometry of trees along gradients of temperature, aridity and competition. Global Ecology and Biogeography 21: 1017–1028.

Lista de Espécies da Flora do Brasil. 2016. Jardim Botânico do Rio de Janeiro; [cited 2016 Jul 17]. Available from: http://floradobrasil.jbrj.gov.br/2016

Lloyd J, Farquhar GD. 2008. Effects of rising temperatures and [CO_2] on the physiology of tropical forest trees. Philosophical Transactions of the Royal Society B: Biological Sciences 363: 1811–1817.

Lopez-Gonzalez G, Lewis SL, Burkitt M, Phillips OL. 2011. ForestPlots.net: a web application and research tool to manage and analyse tropical forest plot data. Journal of Vegetation Science 22: 610–613.

Mantyka-pringle CS, Martin TG, Rhodes JR. 2012. Interactions between climate and habitat loss effects on biodiversity: a systematic review and meta-analysis. Global Change Biology 18: 1239–1252.

Maracahipes L, Marimon BS, Lenza E, Marimon-Junior BH, de Oliveira EA, Mews HA, Gomes L, Feldpausch TR. 2014. Post-fire dynamics of woody vegetation in seasonally flooded forests (impucas) in the Cerrado-Amazonian Forest transition zone. Flora-Morphology, Distribution, Functional Ecology of Plants 209: 260–270.

Marengo JA, Tomasella J, Alves LM, Soares WR, Rodrigues DA. 2011. The drought 800 of 2010 in the context of historical droughts in the Amazon region. Geophysical Research Letters 38.

Marimon BS, Marimon-Junior BH, Feldpausch TR, Oliveira-Santos C, Mews HA, Lopez-Gonzalez G, Lloyd J, Franczak D, de Oliveira EA, Maracahipes L, et al. 2014. Disequilibrium and hyperdynamic tree turnover at the forest–cerrado transition zone in southern Amazonia. Plant Ecology & Diversity 7: 281–292.

McDowell N, Pockman T, Allen CD, Breshears DD, Cobb N, Kolb T, Plaut J, Sperry J, West A, Williams DG. 2008. Mechanisms of plant survival and mortality during drought: why do some plants survive while others succumb to drought? New Phytologist 178: 719–739.

McGarigal K, Cushman S. 2002. Comparative evaluation of experimental approaches to the study of habitat fragmentation effects. Ecological Applications 12: 335–345.

McIntyre PJ, Thorne JH, Dolanc CR, Flint AL, Flint LE, Kelly M, Ackerly DD. 2015. Twentieth-century shifts in forest structure in California: Denser forests, smaller trees, and increased dominance of oaks. Proceedings of the National Academy of Sciences 112: 1458–1463.

NASA 2012. TRMM 3B43(7): Monthly 0.25 x 0.25 degree merged TRMM and other sources estimates, http://disc.sci.gsfc.nasa.gov/precipitation/documentation/TRMM_README/TRMM_3B43_readme.shtml, edited, NASA Distrib. Active Arch. Cent., Goddard Space Flight Cent. Earth Sci., Greenbelt, Md.

Nogueira EM, Fearnside PM, Nelson BW, Barbosa RI, Keizer EWH. 2008. Estimates of forest biomass in the Brazilian Amazon: new allometric equations and adjustments to biomass from wood-volume inventories. Forest Ecology and Management 256: 1853–1857.

Oksanen J, Blanchet FG, Friendly M, Kindt R, Legendre P, McGlinn D, Minchin PR, O'Hara RB, Simpson GL, Solymos P, et al. 2016. vegan: Community Ecology Package. R package version 2.4-0. https://CRAN.R-project.org/package=vegan

Pan Y, Birdsey RA, Phillips OL, Jackson RB. 2013. The structure, distribution, and biomass of the world's forests. Annual Review of Ecology, Evolution, and Systematics 44: 593–622.

Phillips OL, Aragão LEOC, Lewis SL, Fisher JB, Lloyd J, López-González G, Malhi Y, Monteagudo A, Peacock J, Quesada CA, et al. 2009. Drought Sensitivity of the Amazon Rainforest. Science 323:1344–1347.

Phillips OL, Van Der Heijden G, Lewis SL, López-González G, Aragão LE, Lloyd J, Malhi Y, Monteagudo A, Almeida S, Dávila EA, et al. 2010. Drought–mortality relationships for tropical forests. New Phytologist 187: 631–646.

Quinn GP, Keough PR. 2002. Experimental design and data analysis for biologists. Cambridge: Cambridge University Press.

Rangel TF, Diniz-Filho JAF, Bini LM. 2010. SAM: a comprehensive application for spatial analysis in macroecology. Ecography 33: 46–50.

Ratter JA, Richards PW, Argent G, Gifford DR. 1973. Observations on the vegetation of the northeastern Mato Grosso. I. The woody vegetation types of the Xavantina-Cachimbo Expedition area. Philosophical Transactions of the Royal Society of London B 266: 449–492.

Rocha-Santos L, Pessoa MS, Cassano CR, Talora DC, Orihuela RL, Mariano-Neto E, Morante-Filho JC, Faria D, Cazetta E. 2016. The shrinkage of a forest: landscape-scale deforestation leading to overall changes in local forest structure. Biological Conservation 196: 1-9.

Rowland L, da Costa ACL, Galbraith DR, Oliveira RS, Binks OJ, Oliveira AAR, Pullen AM, Doughty CE, Metcalfe DB, Vasconcelos SS, et al. 2015. Death from drought in tropical forests is triggered by hydraulics not carbon starvation. Nature 528: 119–122.

Ryan MG, Binkley D, Fownes JH, Giardina CP, Senock RS. 2004. An experimental test of the causes of forest growth decline with stand age. Ecological Monographs 74: 393–414.

Saatchi SS, Harris NL, Brown S, Lefsky M, Mitchard ET, Salas W, Zuttaa BR, Buermannb W, Lewis SL, Hagenf S, et al. 2011. Benchmark map of forest carbon stocks in tropical regions across three continents. Proceedings of the National Academy of Sciences 108: 9899–9904.

Safriel UN, Volis S, Kark S. 1994. Core and peripheral populations and global climate change. Israel Journal of Plant Sciences 42: 331–345.

Silvério DV, Brando PM, Macedo MN, Beck PS, Bustamante M, Coe MT. 2015. Agricultural expansion dominates climate changes in southeastern Amazonia: the overlooked non-GHG forcing. Environmental Research Letters 10: 104015.

Stegen JC, Swenson NG, Enquist BJ, White EP, Phillips OL, Jørgensen PM, Weiser MD, Monteagudo Mendoza A, Núñez Vargas P. 2011. Variation in above-ground forest biomass across broad climatic gradients. Global Ecology and Biogeography 20: 744–754.

Vlam M, Baker PJ, Bunyavejchewin S, Zuidema PA. 2014. Temperature and rainfall strongly drive temporal growth variation in Asian tropical forest trees. Oecologia 174: 1449–1461.

Way DA, Oren R. 2010. Differential responses to changes in growth temperature between trees from different functional groups and biomes: a review and synthesis of data. Tree physiology 30: 669–688.

Worbes M. 1999. Annual growth rings, rainfall-dependent growth and long-term growth patterns of tropical trees from the Caparo Forest Reserve in Venezuela. Journal of Ecology 87: 391–403.

Zar JH. 2010. Biostatistical analysis. New Jersey: Prentice Hall.

Supplementary material

Table S1. Environmental predictors and vegetation descriptors used in the analyses.

Variable abbreviation	Environmental predictors	Variable abbreviation	Vegetation descriptors
FA	Fragment area (ha)	MIH	Minimum height (m)
DE	Distance to the forest edge (m)	MAH	Maximum height (m)
FC	Forest cover (%)	MH	Median height (m)
MCWD	Maximum climatological water deficit (mm)	H95	Height 95 percentile (m)
Temp	Mean annual temperature (°C)	LH	Weighted Lorey's height
TempMDR	Mean diurnal range (°C)	MD	Median diameter (cm)
Isoter	Isothermality (°C)	MAD	Maximum diameter (cm)
TempSaz	Temperature seasonality (standard deviation *100) (°C)	D95	Diameter 95 percentile (cm)
TempWM	Max temperature of warmest month (°C)	MIA	Minimum allometric ratio (H:D)
TempCM	Min temperature of coldest month (°C)	MAA	Maximum allometric ratio (H:D)
TempAR	Temperature annual range (°C) TempWM - TempCM	MA	Median allometric ratio (H:D)
TempWeQ	Mean temperature of wettest quarter (°C)	A95	Allometric ratio (H:D) 95 percentile
TempDQ	Mean temperature of driest quarter (°C)	MB	Mean biomass (Mg ha)
TempWaQ	Mean temperature of warmest quarter (°C)	MEB	Median biomass (Mg ha)
TempCQ	Mean temperature of coldest quarter (°C)	TB	Total biomass (Mg ha)
Prec	Total annual precipitation (mm)		
PrecWM	Precipitation of wettest month (mm)	-	-
PrecDM	Precipitation of driest month (mm)	-	-
PrecSaz	Precipitation seasonality (Coefficient of Variation) (mm)	-	-
PrecWeQ	Precipitation of wettest quarter (mm)	-	-
PrecDQ	Precipitation of driest quarter (mm)	-	-
PrecWaQ	Precipitation of warmest quarter (mm)	-	-
PrecCQ	Precipitation of coldest quarter (mm)	-	-

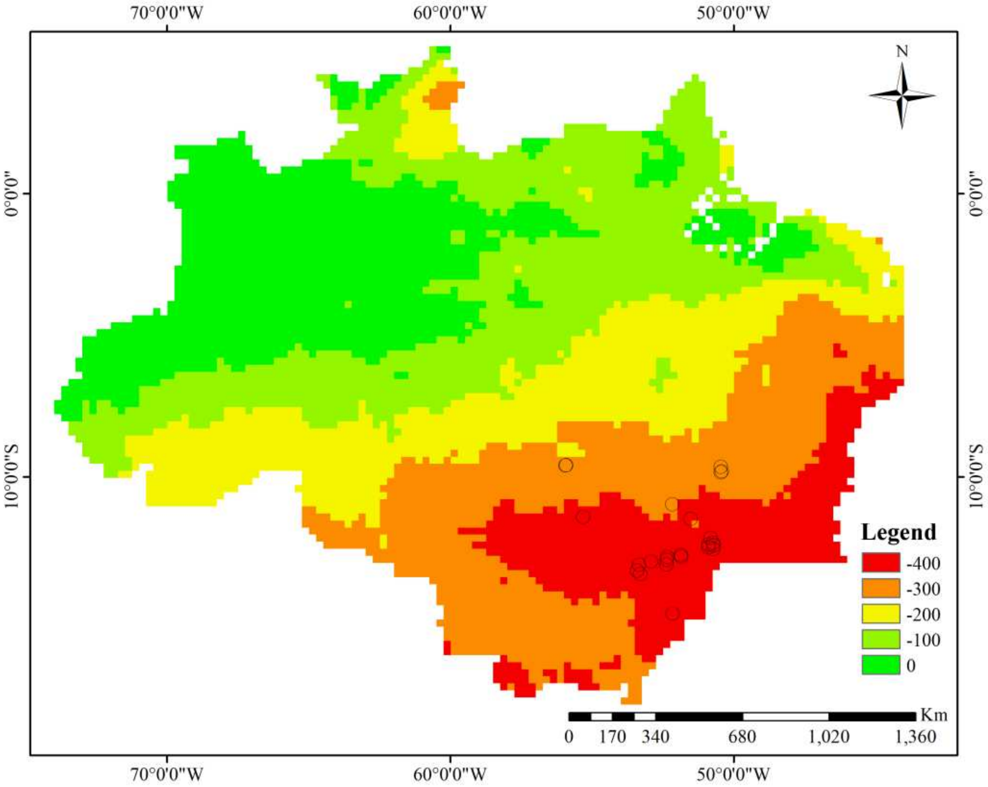

Figure S2. Mean of the maximum climatological water deficit (MCWD) (mm) in the Amazon basin between 1999 and 2011, in the context of the rest of Amazonia. Circles show the forest plots localization.

Table S3. Kendall tau correlations of the all 37 environmental and forest structure variables obtained to the forests of the southern Amazon border. FA = fragment area (ha), DE = distance to the edge (m), MCWD= maximum climatological water deficit (mm), Temp = mean annual temperature (°C), TempMDR = Mean diurnal range (°C), Isoter = Isothermality (°C), TempSaz = Temperature seasonality (standard deviation *100) (°C), TempWM = Max temperature of warmest month (°C), TempCM = Min temperature of coldest month (°C), TempAR = Temperature annual range (°C) TempWM – TempCM, TempWeQ = Mean temperature of wettest quarter (°C), TempDQ = Mean temperature of driest quarter (°C), TempWaQ = Mean temperature of warmest quarter (°C), TempCQ = Mean temperature of coldest quarter (°C), Prec = Total annual precipitation (mm), PrecWM = Precipitation of wettest month (mm), PrecDM = Precipitation of driest month (mm), PrecSaz = Precipitation seasonality (Coefficient of Variation) (mm), PrecWeQ = Precipitation of wettest quarter (mm), PrecDQ = Precipitation of driest quarter (mm), PrecWaQ = Precipitation of warmest quarter (mm), PrecCQ = Precipitation of coldest quarter (mm), MIH = Minimum height (m), MAH = Maximum height (m), MH = Median height (m), H95 = Height 95 percentile (m), LH = Weighted Lorey's height, MD = Median diameter (cm), MAD = Maximum diameter (cm), D95 = Diameter 95 percentile (cm), MIA = Minimum allometric ratio (H:D), MAA = Maximum allometric ratio (H:D), MA = Median allometric ratio (H:D), A95 = Allometric ratio (H:D) 95 percentile, MB = Mean biomass (Mg ha), MEB = Median biomass (Mg ha), TB = Total biomass (Mg ha). Significant correlations ($p \leq 0.05$) are shown in bold type.

	FA	DE	MCWD	Temp	TempMDR	Isoter	TempSaz	TempWM	TempCM	TempAR	TempWeQ	TempDQ	TempWaQ	TempCQ	Prec	PrecWM	PrecDM
FA		**0.55**	**0.61**	-0.18	0.28	-0.17	-0.19	0.17	-0.16	**0.29**	-0.26	0.02	-0.20	-0.01	**0.37**	**0.48**	0.00
DE			**0.51**	-0.21	**0.30**	-0.25	-0.13	0.12	-0.20	**0.32**	**-0.33**	-0.09	-0.23	-0.10	0.23	**0.44**	0.00
MCWD				-0.13	0.24	-0.12	**-0.35**	**0.34**	-0.05	0.24	-0.27	0.13	-0.16	0.08	**0.62**	**0.56**	0.05
Temp					**-0.82**	**0.51**	**-0.42**	**0.32**	**0.92**	**-0.80**	**0.85**	**0.75**	**0.96**	**0.78**	-0.16	**-0.37**	0.17
TempMDR						**-0.64**	0.29	-0.17	**-0.79**	**0.96**	**-0.89**	**-0.59**	**-0.85**	**-0.62**	**0.29**	**0.50**	-0.12
Isoter							**-0.41**	0.20	**0.56**	**-0.69**	**0.66**	**0.62**	**0.54**	**0.63**	-0.18	**-0.46**	0.15
TempSaz								**-0.72**	**-0.51**	**0.29**	-0.27	**-0.68**	**-0.39**	**-0.67**	**-0.30**	-0.09	-0.24
TempWM									**0.39**	-0.15	0.18	**0.57**	**0.30**	**0.55**	**0.43**	0.22	**0.34**
TempCM										**-0.80**	**0.78**	**0.82**	**0.89**	**0.85**	-0.10	**-0.35**	0.22
TempAR											**-0.88**	**-0.59**	**-0.82**	**-0.63**	**0.30**	**0.54**	-0.13
TempWeQ												**0.60**	**0.88**	**0.63**	**-0.30**	**-0.51**	0.09
TempDQ													**0.71**	**0.97**	0.09	-0.17	**0.31**
TempWaQ														**0.74**	-0.19	**-0.40**	0.14
TempCQ															0.05	-0.21	**0.30**
Prec																**0.56**	0.25
PrecWM																	-0.12
PrecDM																	
PrecSaz																	
PrecWeQ																	
PrecDQ																	
PrecWaQ																	
PrecCQ																	
MAH																	
MIH																	
MH																	
H95																	
LH																	
MAD																	
MD																	
D95																	
MAA																	
MIA																	
MA																	
A95																	
MB																	
MEB																	
TB																	

Continuation…

	PrecSaz	PrecWeQ	PrecDQ	PrecWaQ	PrecCQ	MAH	MIH	MH	H95	LH	MAD	MD	D95	MAA	MIA	MA	A95	MB	MEB	TB
FA	**-0.32**	**0.36**	0.16	-0.07	**0.31**	**0.35**	0.23	**0.55**	**0.51**	**0.44**	**0.30**	0.20	0.05	**0.32**	**0.42**	**0.47**	**0.51**	**0.31**	**0.43**	0.20
DE	**-0.30**	**0.29**	0.23	**-0.29**	**0.33**	**0.49**	**0.34**	**0.50**	**0.49**	**0.38**	**0.38**	0.18	0.14	**0.30**	**0.33**	**0.49**	**0.50**	**0.31**	**0.35**	**0.29**
MCWD	**-0.64**	**0.50**	**0.38**	-0.04	**0.48**	**0.39**	**0.42**	**0.57**	**0.46**	**0.51**	**0.46**	0.18	0.12	**0.33**	0.23	**0.56**	**0.56**	**0.32**	**0.44**	0.28
Temp	0.19	**-0.49**	-0.05	0.15	-0.19	**-0.35**	-0.21	**-0.31**	**-0.36**	**-0.35**	-0.23	0.04	**-0.33**	-0.11	**-0.46**	-0.27	**-0.29**	**-0.45**	-0.10	-0.22
TempMDR	**-0.36**	**0.60**	0.16	-0.17	**0.30**	**0.48**	0.22	**0.43**	**0.49**	**0.46**	**0.29**	-0.04	**0.42**	0.17	**0.54**	**0.42**	**0.42**	**0.55**	0.19	**0.37**
Isoter	0.23	**-0.56**	-0.07	**0.37**	-0.27	**-0.43**	-0.08	**-0.34**	**-0.46**	**-0.36**	-0.16	0.03	**-0.39**	-0.21	**-0.46**	**-0.30**	**-0.33**	**-0.45**	-0.12	**-0.33**
TempSaz	0.28	0.03	-0.16	-0.02	-0.18	-0.02	-0.25	-0.19	-0.04	-0.11	-0.17	-0.08	0.16	-0.19	0.14	-0.25	-0.20	0.13	-0.20	-0.13
TempWM	**-0.33**	0.10	0.28	0.03	0.27	0.06	0.18	0.17	0.14	0.14	0.11	0.05	-0.05	0.19	-0.06	0.20	0.16	0.00	0.25	0.22
TempCM	0.15	**-0.43**	0.00	0.11	-0.13	**-0.34**	-0.14	-0.27	**-0.34**	**-0.32**	-0.19	0.04	**-0.36**	-0.06	**-0.43**	-0.23	-0.26	**-0.44**	-0.07	-0.21
TempAR	**-0.35**	**0.63**	0.13	-0.19	**0.31**	**0.50**	0.24	**0.42**	**0.53**	**0.48**	**0.31**	-0.03	**0.45**	0.18	**0.53**	**0.41**	**0.43**	**0.59**	0.22	**0.39**
TempWeQ	**0.36**	**-0.62**	-0.16	**0.29**	**-0.34**	**-0.49**	**-0.29**	**-0.46**	**-0.48**	**-0.47**	**-0.34**	-0.04	**-0.40**	-0.23	**-0.49**	**-0.42**	**-0.43**	**-0.53**	-0.23	**-0.36**
TempDQ	-0.05	**-0.30**	0.10	0.12	0.00	-0.22	-0.01	-0.08	-0.19	-0.14	-0.04	0.09	-0.29	0.01	**-0.35**	-0.04	-0.08	**-0.34**	0.06	-0.12
TempWaQ	0.25	**-0.51**	-0.08	0.19	-0.22	**-0.40**	-0.21	**-0.36**	**-0.38**	**-0.38**	-0.25	0.04	**-0.35**	-0.13	**-0.49**	**-0.31**	**-0.33**	**-0.46**	-0.11	-0.26
TempCQ	-0.02	**-0.34**	0.07	0.15	-0.05	-0.25	-0.02	-0.10	-0.23	-0.18	-0.07	0.06	**-0.33**	-0.01	**-0.37**	-0.05	-0.09	**-0.39**	0.01	-0.13
Prec	**-0.63**	**0.59**	**0.44**	0.11	**0.55**	**0.36**	0.24	**0.44**	**0.50**	**0.50**	0.26	0.11	0.19	**0.30**	**0.31**	**0.39**	**0.40**	**0.39**	**0.36**	**0.39**
PrecWM	**-0.45**	**0.81**	0.20	-0.06	**0.40**	**0.52**	**0.36**	**0.51**	**0.78**	**0.75**	**0.35**	0.03	**0.29**	**0.44**	**0.34**	**0.52**	**0.55**	**0.53**	**0.35**	**0.57**
PrecDM	**-0.29**	-0.12	**0.64**	0.07	**0.44**	0.06	-0.06	-0.03	0.06	-0.01	0.02	0.18	0.05	-0.08	0.02	-0.15	-0.12	0.09	0.08	0.02
PrecSaz		**-0.50**	**-0.62**	0.12	**-0.78**	**-0.38**	**-0.36**	**-0.52**	**-0.43**	**-0.46**	**-0.37**	-0.11	-0.12	-0.26	-0.19	**-0.51**	**-0.47**	-0.27	-0.28	**-0.38**
PrecWeQ			0.22	-0.09	**0.41**	**0.42**	0.28	**0.54**	**0.65**	**0.61**	0.26	0.04	**0.29**	**0.37**	**0.42**	**0.52**	**0.52**	**0.50**	**0.29**	**0.51**
PrecDQ				0.11	**0.75**	0.25	0.11	0.27	**0.32**	0.28	0.16	0.15	0.05	0.13	0.12	0.20	0.20	0.21	0.21	0.21
PrecWaQ					-0.13	-0.20	-0.32	-0.23	-0.06	-0.07	**-0.30**	-0.09	-0.08	-0.16	-0.06	-0.25	-0.20	-0.02	-0.12	-0.04
PrecCQ						**0.40**	**0.33**	**0.42**	**0.49**	**0.41**	**0.30**	0.22	0.15	0.25	0.18	**0.35**	**0.35**	**0.34**	**0.34**	**0.29**
MAH							0.25	**0.42**	**0.68**	**0.68**	**0.55**	-0.03	**0.44**	0.24	**0.33**	**0.38**	**0.40**	**0.54**	0.14	**0.48**
MIH								**0.44**	**0.32**	**0.42**	**0.52**	0.08	0.18	**0.34**	-0.06	**0.47**	**0.51**	0.26	0.29	0.18
MH									**0.46**	**0.56**	**0.31**	0.16	0.15	**0.56**	**0.38**	**0.80**	**0.89**	0.27	**0.47**	**0.38**
H95										**0.78**	**0.42**	0.07	**0.39**	**0.29**	**0.35**	**0.40**	**0.45**	**0.66**	**0.31**	**0.55**
LH											**0.52**	-0.01	**0.41**	**0.45**	0.28	**0.51**	**0.58**	**0.57**	0.27	**0.60**
MAD												0.01	**0.31**	0.19	0.00	**0.35**	**0.35**	**0.39**	0.16	0.25
MD													0.27	0.06	0.09	-0.04	0.06	0.19	**0.58**	-0.22
D95														-0.01	0.15	0.03	0.14	**0.70**	0.28	0.16
MAA															0.18	**0.55**	**0.61**	0.06	0.28	0.28
MIA																**0.30**	**0.31**	**0.32**	0.24	**0.31**
MA																	**0.87**	0.12	**0.30**	**0.32**
A95																		0.24	**0.39**	**0.37**
MB																			**0.35**	**0.39**
MEB																				0.07
TB																				

Table S4. Pre-selected environmental and forest structure variables used in the analyses of the forest-plots of the southern Amazon border. FA = fragment area (ha), DE = distance to the edge (m), FC = forest cover (%), Temp = mean annual temperature (°C), PrecWM = precipitation of wettest month (mm), MCWD= maximum climatological water deficit (mm), MH= median height and H95 = 95 percentile, MD = median diameter and D95 = 95 percentile, MA = median allometric ratio (H:D) and A95 = 95 percentile, MB = mean biomass (Mg), and TB = total biomass.

Forest plots	**Environmental predictors**						**Vegetation descriptors**			
	FA	DE	FC	Temp	PrecWM	MCWD	H95	D95	A95	MB
FEP-01	870	1,030	99	25.5	291	-435.02	20.0	33.6	1.19	0.24
FEP-02	2,035	1,000	100	25.6	289	-435.02	20.1	36.6	1.34	0.25
FEP-03	8,432	990	98	24.9	285	-434.01	19.8	40	1.18	0.27
FEP-04	16,901	520	74	25.1	292	-428.93	20.0	37.8	1.26	0.25
FEP-05	16,901	329	100	25.0	291	-428.93	20.0	37.8	1.29	0.25
FEP-06	45,459	3,600	100	26.9	298	-411.82	22.0	41.4	1.19	0.32
FEP-07	9,789	1,180	100	26.1	309	-397.35	20.5	35.4	1.40	0.25
FES-01	4,968	1,350	78	25.2	274	-468.04	20.4	40.4	1.00	0.31
FES-02	3,499	160	69	24.1	283	-433.5	18.3	39.4	1.32	0.27
FES-03	17,624	90	58	26.7	293	-388.22	21.0	35.4	1.27	0.25
FES-04	13,039	860	88	26.8	289	-388.22	20.8	39.3	1.17	0.31
FES-05	15,680	2,980	100	26.6	278	-387.33	19.3	33.8	1.16	0.24
FOA-01	12,066	900	98	25.1	311	-420.38	25.3	44.8	1.37	0.39
FOA-02	17,628	5,440	100	25.5	390	-342.12	27.8	42.6	1.42	0.43
FOA-03	17,628	5,410	50	25.6	390	-342.12	28.1	42.3	1.37	0.41
FSI -01	21	1	-	27.3	273	-440.57	13.6	32.3	0.93	0.14
FSI -02	378	1	-	27.2	277	-454.52	15.0	35.2	0.92	0.19
FSI -03	164	1	-	27.1	273	-457.47	14.0	24.4	0.99	0.12
FSI -04	605	1	-	27.1	278	-454.52	15.7	28.1	1.02	0.15
FSI -06	5	1	-	27.1	274	-457.47	13.9	40.3	0.75	0.19
FSI -07	8	1	-	27.0	278	-444.82	15.6	45.0	0.77	0.3
FTP-01	234	150	38	24.7	308	-436.02	26.8	51.9	1.14	0.48
FTP-02	29,560	2,720	71	24.9	302	-429.99	22.0	34.7	1.16	0.29
FTP-03	85	80	30	24.7	294	-433.5	24.0	45.3	1.09	0.52

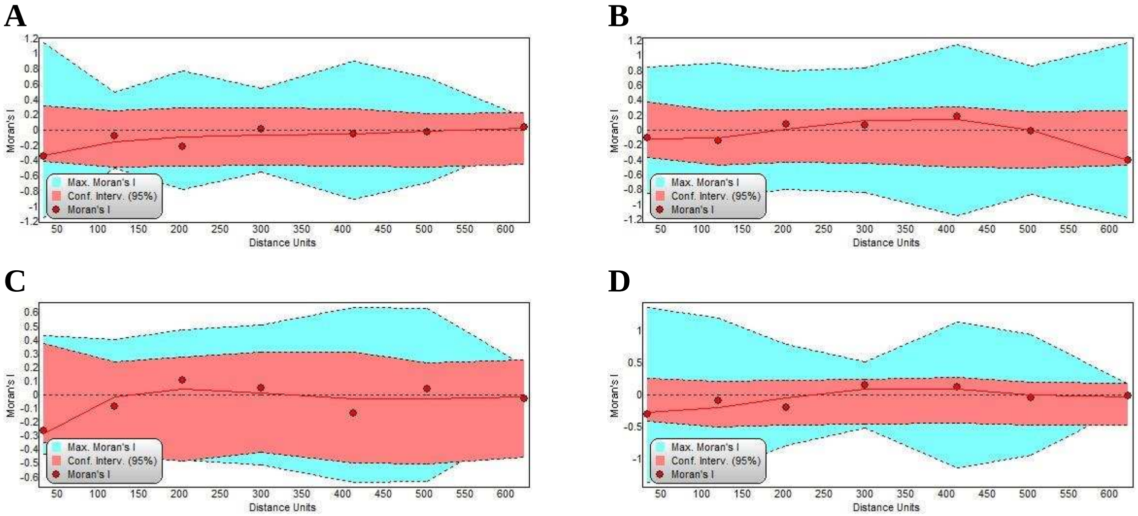

Figure S5. Spatial autocorrelation of the residuals of each model, based in Moran’s I index for: A = height, B = diameter, C= allometric ratio (H:D), and D = biomass of the forests plots in the southern Amazon border.

Table S6. Comparison of the forest structure variables of the forests in the southern Amazon border, based on the Kruskal-Wallis nonparametric analysis of variance (H). MH= median height and H95 = 95 percentile, MD = median diameter and D95 = 95 percentile, MA = median allometric ratio (H:D) and A95 = 95 percentile, MB = mean biomass (Mg), and TB = total biomass. Values on different lines within the same column followed by different letters are significantly different based on Dunnett's post hoc test with the Bonferroni correction.

Forests	**H95**		**D95**		**A95**		**MB**	
FEP-01	19.3	afg	31.5	acd	1.17	aefghi	0.25	adef
FEP-02	19.3	afg	33.1	abcd	1.27	afg	0.25	abdef
FEP-03	19.0	fg	37.5	ab	1.10	deghi	0.27	abdef
FEP-04	19.0	fg	33.9	abcd	1.20	afghi	0.25	abdef
FEP-05	19.7	afg	35.1	abd	1.21	afgh	0.26	abdef
FEP-06	20.4	afg	38.1	ab	1.12	defghi	0.33	abf
FEP-07	19.9	afg	32.8	abcd	1.36	a	0.25	abdef
FES-01	17.6	def	33.8	abcd	0.94	bcd	0.30	abdef
FES-02	18.0	cdef	35.9	ab	1.26	afg	0.28	abef
FES-03	20.1	afg	34.4	abcd	1.19	afghi	0.26	abdef
FES-04	19.6	afg	38.2	ab	1.13	defghi	0.32	abf
FES-05	18.2	ef	31.9	acd	1.12	defghi	0.25	adef
FOA-01	24.0	a	38.8	ab	1.29	afg	0.39	ab
FOA-02	25.7	a	39.4	ab	1.39	a	0.44	ab
FOA-03	24.8	ag	38.3	ab	1.31	af	0.41	ab
FSI-01	13.1	bc	30.5	acd	0.84	bc	0.18	cde
FSI-02	14.2	bcde	31.6	acd	0.85	bc	0.20	cdef
FSI-03	13.1	bcd	24.5	c	0.97	bcd	0.12	c
FSI-04	14.3	bcde	27.0	cd	0.98	bcde	0.16	cd
FSI-05	11.9	b	35.2	ab	0.66	b	0.23	acdef
FSI-06	13.4	bcd	40.5	ab	0.61	b	0.32	abf
FTP-01	23.5	ag	43.2	b	1.06	cdehi	0.47	b
FTP-02	19.7	afg	33.1	abd	1.11	deghi	0.29	abef
FTP-03	21.1	afg	42.8	ab	1.02	bcdei	0.52	abdef

Table S7. Generalized linear models of the factors that influence forest structure of the vegetation in forest plots of the southern Amazon border. Temp = mean annual temperature, MCWD = maximum climatological water deficit, H:D = allometric H:D ratio, FES = seasonal semi-deciduous forest-plots, FOA = open rainforest-plots. Significant effects ($p \leq 0.05$) are shown in bold type.

	Factors	Estimate	Standard	t	P
Height 95 percentile					
	Intercept	2.462	1.229	2.003	0.070
	FES	-0.206	0.177	-1.161	0.270
	FOA	1.848	0.262	7.060	**0.000**
	MCWD	0.007	0.003	2.340	**0.039**
H:D 95 percentile					
	Intercept	8.630	2.679	3.221	**0.007**
	MCWD	0.021	0.007	3.230	**0.007**
	Temp	-0.497	0.230	-2.159	0.052